Tribol Lett (2014) 54:287–295
DOI 10.1007/s11249-014-0321-4

ORIGINAL PAPER

Contact Stress-Induced Micromagnetic Behavior in Magnetic Recording Disk

Lei Yang · Dongfeng Diao

Received: 22 October 2013 / Accepted: 10 March 2014 / Published online: 21 March 2014

Abstract Stress plays an important role in the magnetic properties of ferromagnetic materials. Sliding contact in hard disk drives can lead to tribological failures of the disk in terms of data loss and demagnetization. However, the relationship between contact stress-induced magnetization changes and tribological failures of magnetic recording disk is rarely discussed. In this study, the contact stress-induced micromagnetic behavior in magnetic recording disk was investigated using micromagnetic simulation. A micromagnetic model including the magnetostriction effect into the Landau–Lifshitz–Gilbert equation was developed to simulate the stress effect on the magnetization changes. Then finite element analysis was used to calculate the critical stresses for the occurrence of data loss and demagnetization of perpendicular magnetic recording disk under sliding contact according to our previous experimental results. Based on these simulation results, it was found that the magnetic moment decreased by 8.9 % under the critical stress for data loss, and it rotated 55.7° under the critical stress for demagnetization. In addition, the simulated static domain structures when data loss and demagnetization occur were in agreement with the previously reported experimental results. Finally, the relationship between the contact stress-induced tribological failures and micromagnetic behavior of the magnetic disk was illustrated. It was proposed that data loss is caused by the magnetization reduction, while demagnetization is caused by the magnetization rotation.

Keywords Micromagnetic simulation · Contact stress · Magnetization changes · Finite element analysis · Data loss · Demagnetization

1 Introduction

In order to achieve higher areal recording density, the carbon overcoat thickness on the surface of a magnetic recording disk and the flying height of a magnetic recording head must be reduced [1–3], increasing the possibility of head/disk interface contacts. These contacts can lead to data loss and demagnetization of the magnetic disk. A number of studies have been published on this subject. Suk et al. [4] investigated the head/disk contact-induced magnetic data loss during load/unload process. Roy et al. [5] found that the interactions of particles with a head/disk interface could lead to permanent loss of data in the recording disk. Lee et al. [6] believed that demagnetization of the magnetic recording disk was related to the plastic strain in the recording layer. Xu et al. [7] observed a decrease in the magnetic coercivity and anisotropy in the scratch area of a magnetic disk. Talke et al. [8] studied the magnetic information erasure due to transient slider/disk contacts. In our recent work [9], drive-level tests of diamond tips sliding against perpendicular magnetic recording (PMR) disks were performed. By using magnetic head scanning and magnetic force microscopy (MFM), the critical normal forces and sliding velocities for data loss and demagnetization of PMR disk under sliding contact were obtained. It was found the critical normal forces for data loss and demagnetization under sliding velocity of

L. Yang
Key Laboratory of Education Ministry for Modern Design and Rotor-Bearing System, School of Mechanical Engineering, Xi'an Jiaotong University, Xi'an 710049, China

D. Diao (✉)
Institute of Nanosurface Science and Engineering (INSE), Shenzhen University, Shenzhen 518060, China
e-mail: dfdiao@szu.edu.cn

20.36 m/s were 0.02 and 8 mN, respectively. But the micromagnetic mechanisms of data loss and demagnetization under sliding contact are still unclear.

As we know, stress plays an important role in the magnetic properties of ferromagnetic materials. Experimental and theoretical researches have been devoted to investigate the influence of stress on magnetization [10–12]. Micromagnetic simulation is an effective way to study the magnetic properties under stress. A magnetostriction model has been developed by Jiles [13] to describe stress effect on magnetic properties of bulk materials. Based on this model, a lot of researchers have studied the stress-induced magnetization changes. Zhu et al. [14] calculated the magnetization curves of a nickel thin film under applied stress and found the shape of the hysteresis loop and the magnetic properties changed systematically. Li et al. [15] proposed a modified micromagnetic model to investigate the asymmetrical magnetic properties under tension and compression. However, the relationship between stress-induced magnetization changes and tribological failures of magnetic recording disk was rarely discussed. Therefore, further study is needed on this subject.

The aim of this paper is to investigate the micromagnetic mechanism of sliding contact-induced data loss and demagnetization in the magnetic recording disk. Micromagnetic simulation was used to investigate the effect of stress on the magnetization changes of the recording medium. Then finite element analysis (FEA) was used to calculate the critical stresses for the occurrence of data loss and demagnetization according to our previous experimental results. Finally, the mechanisms of data loss and demagnetization of perpendicular magnetic recording disk under sliding contact were discussed on the basis of the simulation results.

2 Micromagnetic Simulation

2.1 Micromagnetic Model

The magnetic moment in the magnetic material will alter its magnitude and direction when sliding contact induces a stress field at the magnetic domain, which is called magnetostriction effect. The amount of the changes depends on the magnetostriction coefficient as well as the stress induced by sliding contact. Although the magnetostriction effect is small in most magnetic materials, the existence of it can have a substantial effect on the magnetic properties, especially when the stress becomes large enough. In order to investigate the stress-induced magnetization changes in the magnetic recording layer, a micromagnetic model was developed considering the magnetostriction effect.

When the magnetic material is under applied stress, the magnetostriction energy has to be included in the total Gibbs free energy E, which can be written as following:

$$E = E_{\text{ext}} + E_{\text{exch}} + E_{\text{anis}} + E_{\text{demag}} + E_{\text{ms}} \quad (1)$$

where E_{ext} is the energy contribution due to an external field, which is also called Zeeman energy. E_{exch} is the exchange energy, which is the energy for forming a magnetic domain wall. E_{anis} is the magnetocrystalline anisotropy energy, which is the energy barrier preventing the magnetization deviates from the preferred directions. E_{demag} is the demagnetizing energy, which is generated by long range interactions. E_{ms} is the magnetostriction energy. When the magnetostriction is isotropic, the magnetostriction energy can be given by:

$$E_{\text{ms}} = -\frac{3}{2}\lambda\sigma\cos^2\theta \quad (2)$$

where λ is the magnetostriction constant, σ is the applied stress, and θ is the angle between the magnetic moment and the applied stress. The equilibrium magnetization configuration of the magnetic recording layer under stress can be found by minimizing the total Gibbs free energy.

Figure 1 shows the three-dimensional micromagnetic model. The simulation was performed with uniaxial anisotropy energy function. The initial magnetization state (M) was assumed to be two equal-sized antiparallel domains along the anisotropy axis separated by a 180° Bloch wall at the center line. According to the characteristics of the studied perpendicular magnetic recording disk, the dimension of the micromagnetic model was 80 nm × 40 nm with thickness of 30 nm. The width of the domain wall was 4 nm. The easy axis and the initial magnetization were both along the normal direction of the disk surface (y axis). The compressive stresses were applied on the film along x axis, y axis and z axis, respectively. In this study, the micromagnetic simulation was done by using finite element method, in which the

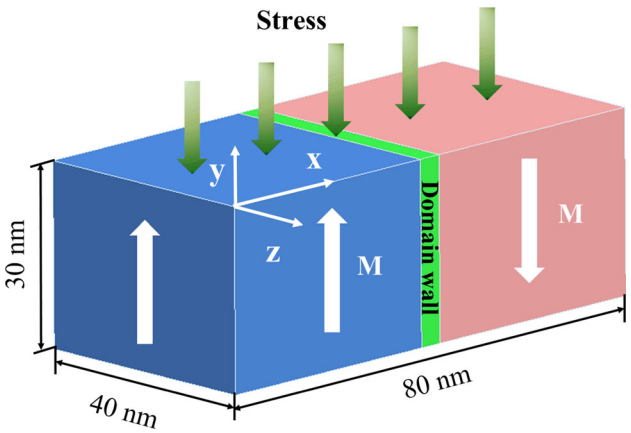

Fig. 1 The three-dimensional micromagnetic model

model needs to be discretized with finite element. The magnetization within each element was assumed to be uniform and represented by a single magnetic moment. The finite element mesh of the model was generated by using Gmsh. The model was composed of four-node regular tetrahedron elements. The mesh size was 2 nm, which is larger than the atomic diameter and smaller than the exchange length. The material properties of the magnetic recording medium were given as: $J_s = 1.5$ T, $K_1 = 0.6 \times 10^6$ J/m^3, $A = 2.7 \times 10^{-11}$ J/m, $\lambda = 20 \times 10^{-6}$ [16, 17], where J_s is the saturation magnetic polarization, K_1 is the first magnetocrystalline anisotropy constant, and A is the exchange constant. The finite element mesh and the material properties were then input into the public domain software Magpar, a parallel finite element micromagnetics package [18]. The damping constant was assumed to be 0.1 in the simulation, and the thermal effects were not taken into account.

Figure 2 gives the simulated hysteresis loop of the magnetic media based on the above magnetic parameters used in the micromagnetic model. The external field was along the y axis, perpendicular to the media surface. The simulated coercivity of the magnetic recording layer was around 476.4 kA/m, which was close to the typical coercivity value of the perpendicular magnetic recording media.

2.2 Micromagnetic Simulation Results

Based on this model, the equilibrium magnetization configurations of the magnetic recording layer under different stresses were obtained. Then the direction and magnitude changes of the magnetic moment in each domain were calculated. In this paper, the x, y and z components of the magnetization moment of each domain were given by averaging the magnetic moments of all the nodes inside the domain.

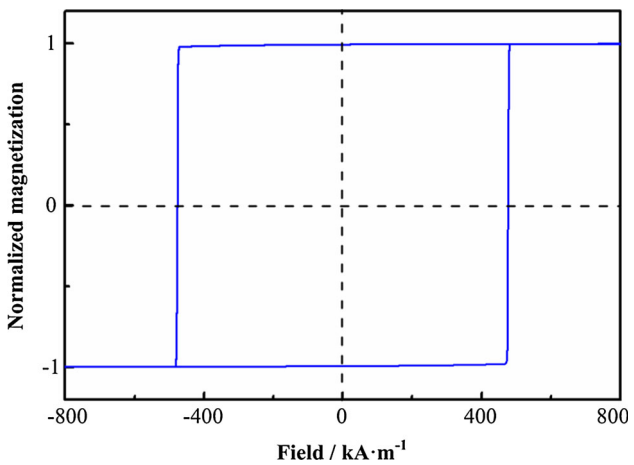

Fig. 2 Simulated hysteresis loop of the perpendicular magnetic recording media

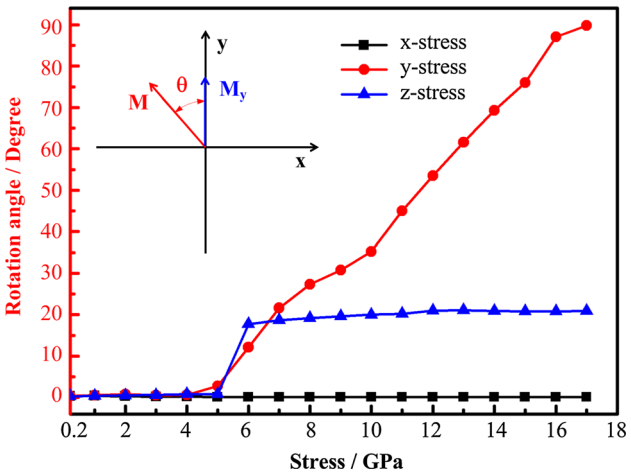

Fig. 3 The effect of stress on the magnetic moment rotation angle

From the simulation results, it was found that the magnetic moment rotated in the x–y plane under compressive stress. Figure 3 gives the curve in relation to the rotation angle in x–y plane and the compressive stress in different directions. It can be seen that the rotation angle remains 0 as the x axis stress increases, which means that the magnetic moment does not rotate when the compressive stress is applied along x axis. However, the magnetic moment begins to rotate at a stress level of 5 GPa when the applied stresses are in y axis and z axis. In addition, the rotation angle increases with the increase in the y axis stress, while it keeps constant around 20° as the z axis stress increases. These results indicate that the direction of the stress has effect on the stress-induced magnetization changes. When the stress is in the same direction with magnetization, it can cause larger changes of the magnetization. This is in accordance with the expectation mentioned in Jeong's work [19]. Thus, in the following of this paper, the magnetization changes refer to the y axis stress-induced magnetization changes. For the different effect of x axis stress and z axis stress on the rotation angle, it is also caused by the direction relation between stress and magnetization. As mentioned above, the domain wall in this micromagnetic model is 180° Bloch wall, in which the magnetization changes gradually from positive y direction to negative y direction in the y–z plane. Therefore, parts of the magnetic moments in the domain wall are in the same direction with the z axis stress. As a result, when the z axis stress increases large enough, it can cause magnetization changes in the domain wall, which interacts with other magnetic moments and leads to magnetization changes in the whole domain.

From Fig. 3, it is also found that the rotation angle finally increases to 90° with the increase in the y axis stress.

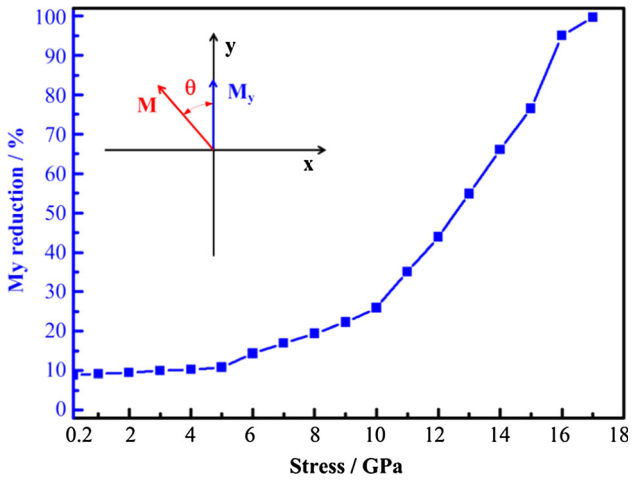

Fig. 4 The effect of stress on the magnetization reduction

As it is known, the direction of the magnetization moment is mainly controlled by the magnetocrystalline anisotropy in the absence of stress. However, when a stress is applied on the magnetic material, the direction of the magnetization moment is controlled by both stress and magnetocrystalline anisotropy. Therefore, when the stress is less than 5 GPa, the magnetization moment does not rotate since the stress-induced anisotropy is not strong enough to control the magnetization moment. But when the stress increases high enough, the magnetization moment will be dominated by the stress-induced anisotropy.

Because the studied disk is a perpendicular recording disk, the recording data are related to the magnetization component along the normal direction of the disk surface (y axis). Thus, the y-component magnetization (M_y) changes under compressive stress were calculated. It was observed that M_y decreased under the compressive stress. Figure 4 shows the curve in relation to M_y reduction and the applied stress. It can be seen that M_y reduction increases with the increase in the applied stress. The reduction increases abruptly when the stress is above 5 GPa. This is in accordance with the above result as shown in Fig. 3. Because when the stress increases above 5 GPa, the magnetization moment begins to rotate, which leads to the decrease in the magnetization along the y axis. From the above micromagnetic simulation results, it was found that when a stress is applied on the perpendicular magnetic recording disk, the magnetic moment first decreased and then it began to rotate with the increase in stress.

3 Mechanism of Data Loss and Demagnetization

The above micromagnetic simulation results suggest that contact stress can lead to magnetization rotation and reduction in the recording layer. In order to further correlate such micromagnetic behavior with tribological failures of magnetic disk, the critical stresses for data loss and demagnetization under sliding contact were calculated, and the magnetization changes under the critical stress were discussed.

3.1 Finite Element Model

According to our previous experimental results on PMR disk with areal recording density of 329 Gb/in^2, the critical normal force (W) for data loss was 0.02 mN under sliding velocity (V) of 20.36 m/s, and the critical normal force for demagnetization was 8 mN under sliding velocity of 20.36 m/s. To obtain the critical stresses for the data loss and demagnetization of PMR under sliding contact, finite element model using thermomechanical coupling was developed to calculate the stress distribution in the disk. Two different FEA models were utilized: data loss model and demagnetization model.

In the data loss model, both surfaces of the diamond tip and the magnetic disk were rough. Due to the Greenwood and Williamson model, the contact between the diamond tip and the magnetic disk can be converted to the contact between a smooth disk surface and a tip surface with spherically shaped asperities with a uniform mean radius, as shown in Fig. 5. The combined roughness parameters were given as [20]: $r = 5.452$ μm, $\eta = 7.177$ μm^{-2}, $\sigma = 1.245$ nm, where r is the mean radius of curvature of asperity, η is the areal density of asperities, and σ is the standard deviation of surface heights. Then the contact state can be determined by calculating the plasticity index ψ:

$$\psi = \frac{E'}{H}\sqrt{\frac{\sigma}{r}} \tag{3}$$

$$E' = \left[\frac{(1-v_b^2)}{E_b} + \frac{(1-v_d^2)}{E_d}\right]^{-1} \tag{4}$$

where E' is the composite Young's modulus; E_b and E_d are the Young's modulus of the diamond tip and the magnetic disk, respectively; v_b and v_d are the Poisson ratio of the diamond tip and the magnetic disk, respectively; and H is the hardness of the softer material. If $\psi < 0.6$, the contact is elastic; if $\psi > 1.0$, the contact is plastic. In this paper, the following values were used to obtain the plasticity index: $E_b = 1{,}000$ GPa, $E_d = 180$ GPa, $v_b = 0.2$, $v_d = 0.3$, $H = 7.9$ GPa [21]. The calculated value of ψ was 0.32, suggesting that the contact between the diamond tip and the disk is elastic. Based on this model, the contact parameters for the development of the finite element model were calculated. The details of the calculation have been introduced in our previous paper [22]. Meanwhile, since the contact is elastic, the asperity on the tip surface can be

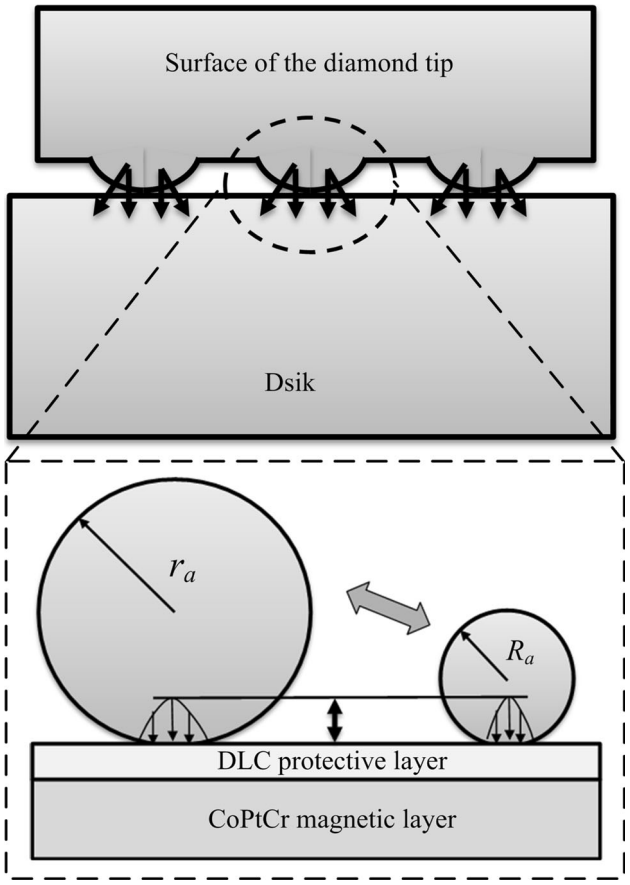

Fig. 5 Data loss contact model

changed from micrometer scale (r) to nanometer scale (R) with the equivalent pressure distribution according to Hertz elastic contact theory. The respective normal force loaded on the nanometer scale asperity (W_R) can be given:

$$W_R = W_r \left(\frac{R}{r}\right)^2 \tag{5}$$

where W_r is the respective normal force loaded on the micrometer scale asperity.

In the demagnetization model, the equivalent roughness was not considered since plastic deformation occurred during the demagnetization test. The contact pair was formed between the diamond tip surface and the magnetic disk surface.

Figure 6 shows the three-dimensional finite element model of an analytical rigid sphere surface loading against a layered magnetic disk. In the data loss model, the radius of the sphere was assumed to be 80 nm, representing the asperity on the tip. The layered disk structure was assumed to be a deformable and semi-infinite half-space with dimensions of 800 nm (x direction) × 34 nm (y direction) × 40 nm (z direction). The demagnetization model also consisted of an analytical rigid surface and a layered magnetic disk. The radius of the rigid surface was 5 μm, representing the diamond tip. The dimension of the layered magnetic disk was 2,000 nm (x direction) × 34 nm (y direction) × 600 nm (z direction). As the stress distribution in the magnetic recording layer (MAG) is mainly concerned in this paper, the layered disk model was only composed of 4 nm DLC protective layer and 30 nm CoPtCr magnetic layer. The deformable mesh was composed of eight-node trilinear hexahedral elements with full integration and thermomechanical coupling. The mesh was finest close to the contact region and coarsest away from the region of interest. Since the problem is symmetric with respect to the plane, we consider only one half of the disk as shown in Fig. 6. The spherical slider was modeled as a rigid body using an analytical rigid surface to ensure a smooth contact surface as well as to reduce the computational time.

Table 1 shows the detailed physical and material properties of the finite element model [21, 23]. In the data loss model, an elastic material constructive law was used. In the demagnetization model, a bilinear elastic–plastic material constructive law with a tangent modulus was used for MAG [24], with the value as listed in Table 1.

For the boundary conditions, the rigid surface was constrained from rotating. The nodes on the left and right sides of the disk were constrained from moving along the x direction. The nodes at the bottom of the disk were constrained from moving along the y direction. The back side of the disk was constrained from moving along the z direction, and symmetric constrain was applied on the front side of the disk. Moreover, all the above surfaces were thermally insulated.

In the analysis, the respective critical normal forces and sliding velocities were applied on the rigid surface. Sliding was taken along the positive x direction. The heat generated during a contact was assumed to be equal to the dissipated frictional energy and was divided between the sphere and the disk. The friction coefficient was 0.24 in the data loss test and 0.06 in the demagnetization test.

3.2 Analysis of Stress-Induced Data Loss and Demagnetization

According to the micromagnetic simulation results, the contact stress can lead to magnetization changes of the magnetic recording disk, and the same directions of the stress and magnetization can cause larger magnetization changes. So the y axis stress was taken to evaluate the critical stresses for data loss and demagnetization in this paper.

Figure 7a gives the contours of the y axis stress in the recording layer of the magnetic disk under critical condition for data loss ($W = 0.02$ mN, $V = 20.36$ m/s). The

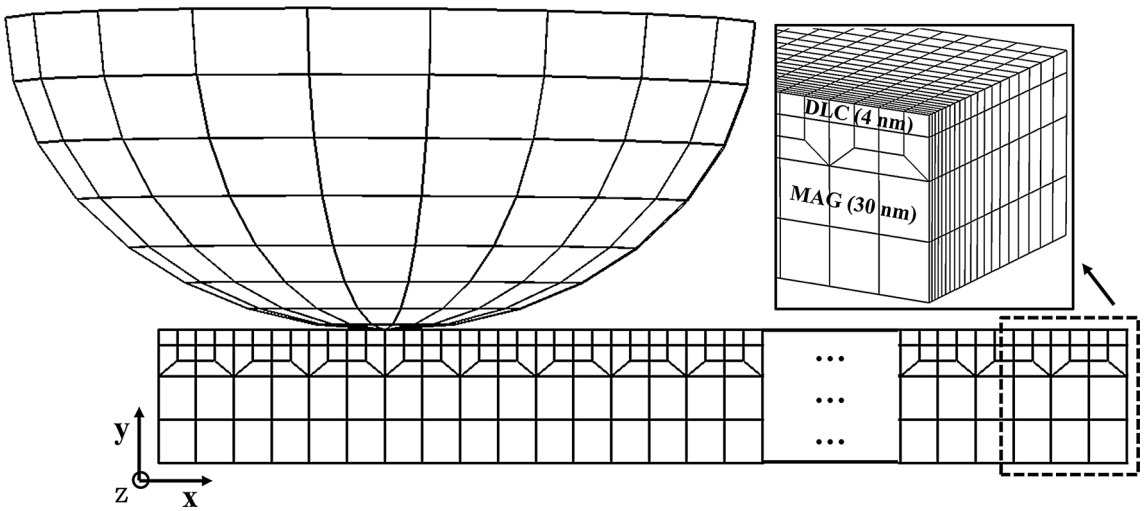

Fig. 6 Illustration of finite element model

Table 1 Material properties used in the finite element analysis

Properties	DLC	MAG
Poisson's rate	0.3	0.3
Young's modulus (E/GPa)	180	210
Yield stress (σ_y/GPa)	13	3.4
Tangent modulus (E_T/GPa)	–	20
Thermal expansion coefficient ($\beta/10^{-6}$ K^{-1})	6.95	12.50
Thermal conductivity [k/W(m K)$^{-1}$]	1.24	6.03
Specific heat [c/J(kg K)$^{-1}$]	950	340
Density ($\rho/10^3$ kg m^{-3})	2.10	12.67

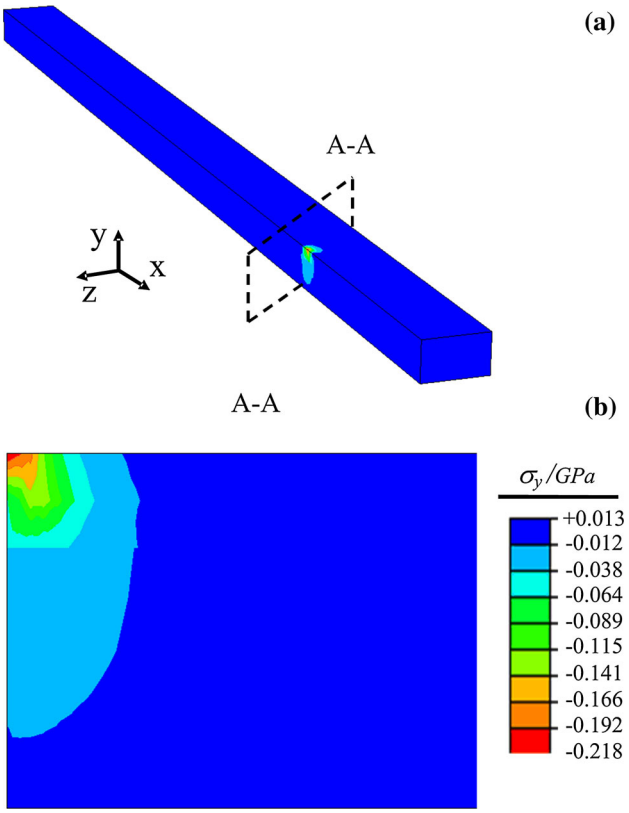

Fig. 7 **a** Contours of the y axis stress in the magnetic recording layer; **b** cross-sectional view at the position of the maximum stress

position of the maximum stress is at the end of the sliding track. Figure 7b shows the cross-sectional view of stress distribution at the position of the maximum stress, and the maximum stress occurs at the top of the recording layer, which is a compressive stress with the value of 0.218 GPa. Thus, the critical stress for data loss is defined here as the maximum compressive stress in the magnetic recording layer, $\sigma_{\text{Data loss}} = 0.218$ GPa. In Jiang's study [22], the critical stress for data loss of PMR disk with areal recording density of 101 Gb/in^2 was 0.517 GPa. In comparison with Jiang's result, it suggests that the critical stress for data loss decreases with the increase in the areal recording density of the PMR disk.

Figure 8a gives the contours of the equivalent plastic strain in the recording layer of the magnetic disk under critical condition for demagnetization ($W = 8$ mN, $V = 20.36$ m/s). It shows that plastic deformation occurs in the recording layer under the critical condition. The position of the maximum strain is at the end of the sliding track. The value of the maximum strain is 31.9 %. According to our previous experimental results, the plastic strain in the recording layer is about 30.7 % under normal force of 8 mN with sliding velocity of 20.36 m/s, indicating that the FEA result compares well with the experimental results. Figure 8b shows the contours of y axis stress in the recording layer under the critical condition. The maximum stress also occurs at the end of the sliding track, which is a

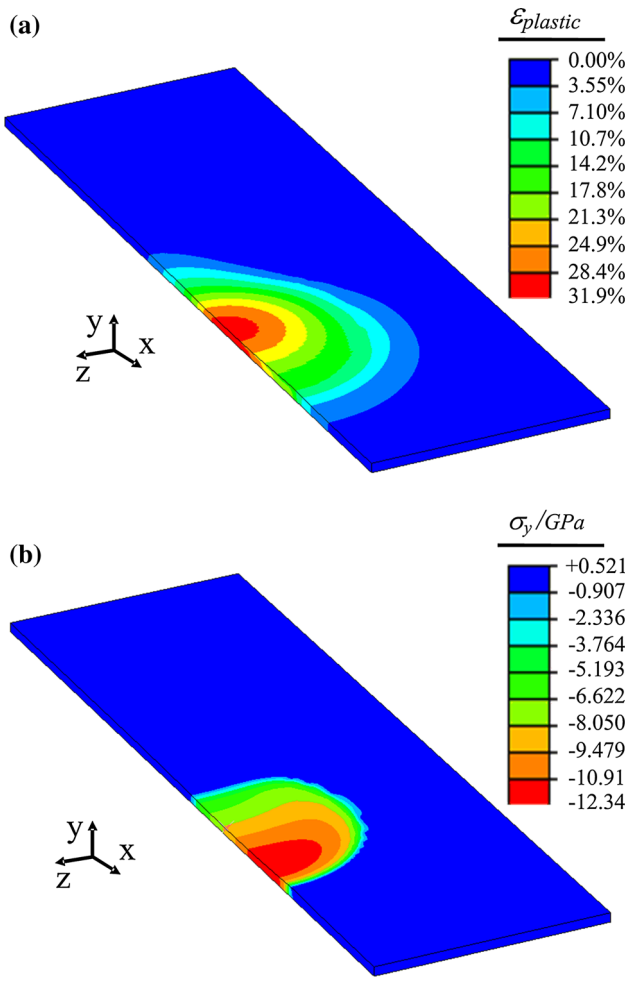

Fig. 8 **a** Contours of the equivalent plastic strain in the magnetic recording layer; **b** contours of *y* axis stress in the magnetic recording layer

compressive stress with the value of 12.34 GPa. Thus, the critical stress for demagnetization is defined here as the maximum compressive stress in the magnetic recording layer, $\sigma_{\text{Demagnetization}} = 12.34$ GPa.

Through the finite element analysis, the critical stresses for the occurrence of data loss and demagnetization of PMR disk under sliding contact were obtained. And based on the above micromagnetic simulation results, it was found that the magnetization reduced by 8.9 % under the critical stress for data loss, and it rotated 55.7° under the critical stress for demagnetization. In order to further study how the magnetic domains change when data loss and demagnetization occur, the static magnetic domain structures under the critical stresses of data loss and demagnetization were obtained through the above micromagnetic simulation. Figure 9a, b shows the simulation results of the static magnetic domain structures under the critical stresses of data loss and demagnetization. As shown in the figure, the two antiparallel domain structures can be clearly observed under the critical stress of data loss while it looks blurry under the critical stress of demagnetization. In our previously reported experimental work, it was found that the magnetic domains did not change in the sliding contact area when data loss occurred, while the magnetic domains could not be clearly observed when demagnetization occurred (as shown in Fig. 9c, d). This suggests that the simulation results are in accordance with the experimental results. Therefore, based on the above simulation results, the tribological failures observed in the previous experiments are correlated with the contact stress-induced magnetization changes. To be specific, data loss is mainly caused by the magnetization reduction, and demagnetization is mainly caused by the magnetization rotation.

4 Discussion

In the present study, the mechanisms for data loss and demagnetization have been clarified to be caused by the stress-induced magnetization changes using micromagnetic simulation. In addition, there is an interesting point in which we found the critical stress for data loss decreased as the areal recording density increased compared with the previous study. It is known that the domain size and the thickness of the magnetic recording layer need to be reduced as the demands of areal recording density are higher [25]. This could probably affect the occurrence of data loss and demagnetization under sliding contact. Therefore, the effects of domain size and the recording layer thickness on the stress-induced magnetization changes were discussed.

Figure 10 shows the effect of domain size in the magnetic recording layer on the rotation angle and M_y reduction (under 12.34 GPa). As shown in the figure, when the domain size is below 30 nm, the rotation angle and M_y reduction decrease with the increase in the domain size. But when the domain size increases up to 30 nm, the rotation angle and M_y reduction increase with the increase in domain size. This indicates that the stress-induced magnetization changes will be worse as the domain size decreases below 30 nm, which could increase the probability for the occurrence of data loss and demagnetization.

Figure 11 shows the effect of magnetic recording layer thickness on the rotation angle and M_y reduction (under 12.34 GPa). It can be found that the rotation angle and M_y reduction decrease with the increase in the magnetic recording layer thickness. This indicates that data loss and demagnetization could more easily occur under sliding contact as the thickness of the magnetic recording layer decreases.

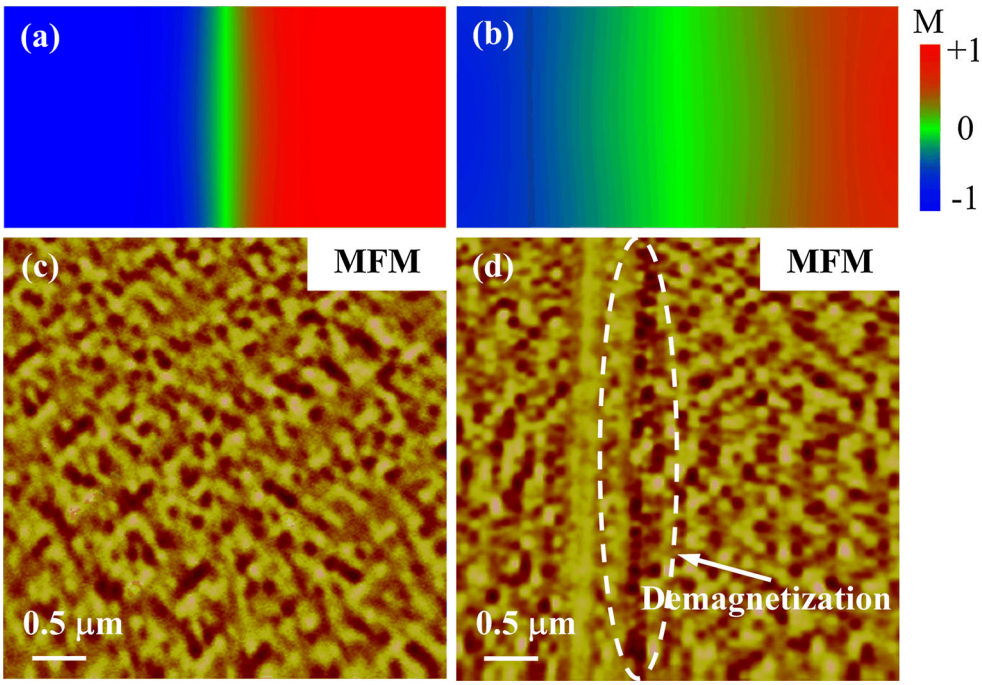

Fig. 9 **a** Simulated static magnetic domain structure under critical stress of data loss; **b** simulated static magnetic domain structure under critical stress of demagnetization; **c** MFM image in the data loss area; **d** MFM image in the demagnetization area (**c**, **d** from Ref. [9])

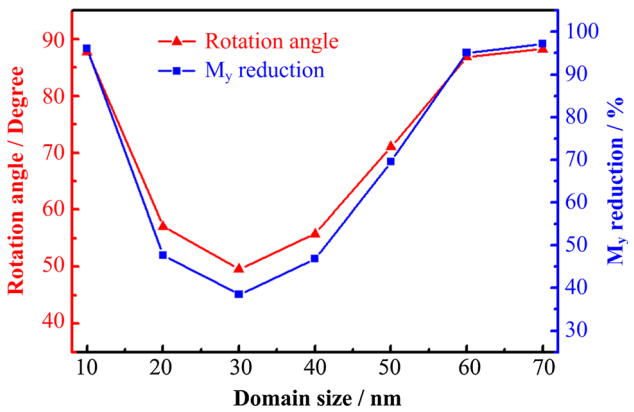

Fig. 10 The effect of domain size on the stress-induced magnetization changes (under 12.34 GPa)

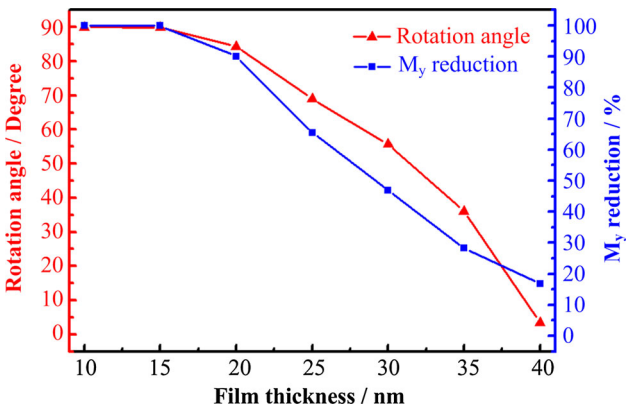

Fig. 11 The effect of film thickness on the stress-induced magnetization changes (under 12.34 GPa)

5 Conclusion

In conclusion, micromagnetic simulations have been performed to study the contact stress-induced micromagnetic behavior in perpendicular magnetic recording disk under sliding contact. The magnetization changes under different stresses were calculated. The results showed that the same directions of the applied stress and magnetization could cause larger magnetization changes. Then the critical stresses for the occurrence of data loss and demagnetization were evaluated by using finite element analysis based on the previous experimental results. Thereafter, the correlation between stress-induced magnetization changes and the tribological failures in perpendicular magnetic recording disk was discussed. It was found that the magnetization reduced by 8.9 % under the critical stress for data loss, and it rotated 55.7° under the critical stress for demagnetization. Furthermore, the simulated static magnetic domain structures when data loss and demagnetization occur agreed with the previous experimental results. Finally, tribological failures of magnetic disk under sliding contact were correlated with the contact stress-induced micromagnetic behavior. It was proposed that data loss is caused by the magnetization reduction, and demagnetization is caused by the magnetization rotation.

Acknowledgments The authors would like to thank the National Nature Science Foundation of China under Grant Numbers of 51175405 and 51305332, Research Fund for the Doctoral Program of Higher Education of China under Grant Number of 20120201110029, and the National Nature Science Foundation Major Research Program on Nanomanufacturing under Grant Number of 91323303.

References

1. Samad, M.A., Rismani, E., Yang, H., Sinha, S.K., Bhatia, C.S.: Overcoat free magnetic media for lower magnetic spacing and improved tribological properties for higher areal densities. Tribol. Lett. **43**, 247–256 (2011)
2. Zhang, H.S., Komvopoulos, K.: Surface modification of magnetic recording media by filtered cathodic vacuum arc. J. Appl. Phys. **106**, 093504 (2009)
3. Zhou, W.D., Liu, B., Yu, S.K., Hua, W.: Inert gas filled head–disk interface for future extremely high density magnetic recording. Tribol. Lett. **33**, 179–186 (2009)
4. Suk, M., Jen, D.: Potential data loss due to head/disk contacts during dynamic load/unload. IEEE Trans. Magn. **34**, 1711–1713 (1998)
5. Roy, M., Brand, J.L.: Soft particle-induced magnetic erasure without physical damage to the media. ASME J. Tribol. **129**, 729–734 (2007)
6. Lee, S.C., Hong, S.Y., Kim, N.Y., Ferber, J., Che, X.D., Strom, B.D.: Stress induced permanent magnetic signal degradation of perpendicular magnetic recording system. ASME J. Tribol. **131**, 011904 (2009)
7. Xu, J.G., Furukawa, M., Nakamura, A., Honda, M.: Mechanical demagnetization at head disk interface of perpendicular recording. IEEE Trans. Magn. **45**, 893–898 (2009)
8. Ovcharenko, A., Yang, M., Chun, K., Talke, F.E.: Simulation of magnetic erasure due to transient slider-disk contacts. IEEE Trans. Magn. **46**, 770–777 (2010)
9. Yang, L., Diao, D.F., Zhan, W.J.: Data loss and demagnetization of perpendicular magnetic recording disk under sliding contact. Tribol. Lett. **46**, 329–335 (2012)
10. Perevertov, O.: Influence of the residual stress on the magnetization process in mild steel. J. Phys. D Appl. Phys. **40**, 949–954 (2007)
11. Lo, C.C.H.: Experimental and modeling studies of the magnetomechanical effect in substituted cobalt ferrites for magnetoelastic stress sensors. J. Appl. Phys. **107**, 09E706 (2010)
12. Jin, K., Kou, Y., Liang, Y., Zheng, X.: Effects of hysteresis losses on dynamic behavior of magnetostrictive actuators. J. Appl. Phys. **110**, 093908 (2011)
13. Jiles, D.C.: Theory of the magnetomechanical effect. J. Phys. D Appl. Phys. **28**, 1537–1546 (1995)
14. Zhu, B., Lo, C.C.H., Lee, S.J., Jiles, D.C.: Micromagnetic modeling of the effects of stress on magnetic properties. J. Appl. Phys. **89**, 7009–7011 (2001)
15. Li, J., Xu, M.: Modified Jiles-Atherton-Sablik model for asymmetry in magnetomechanical effect under tensile and compressive stress. J. Appl. Phys. **110**, 063918 (2011)
16. Im, M.Y., Jeong, J.R., Shin, S.C.: Saturation magnetostriction coefficient measurement of CoCrPt alloy thin films using a highly sensitive optical deflection-detecting system. J. Appl. Phys. **97**, 10N110 (2005)
17. Xia, W., Xiao, C., Shindo, D.: Changes of magnetic anisotropy of CoPtCr perpendicular films due to Ru intermediate layer under high gas pressure. IEEE Trans. Magn. **46**, 3711–3714 (2010)
18. Scholz, W., Fidler, J., Schrefl, T., Suess, D., Dittrich, R., Forster, H., Tsiantos, V.: Scalable parallel micromagnetic solvers for magnetic nanostructures. Comp. Mat. Sci. **28**, 366–383 (2003)
19. Jeong, T.G., Bogy, D.B.: Dynamic loading impact-induced demagnetization in thin film media. IEEE Trans. Magn. **29**, 3903–3905 (1993)
20. Suh, A.Y., Polycarpou, A.A.: Adhesive contact modeling for sub-5-nm ultralow flying magnetic storage head-disk interfaces including roughness effects. J. Appl. Phys. **97**, 104328 (2005)
21. Bhushan, B.: Magnetic head-media interface temperatures—part 3: application to rigid disks. ASME J. Tribol. **114**, 420–430 (1992)
22. Jiang, W.F., Diao, D.F.: The critical conditions for tribo-demagnetization of perpendicular magnetic recording disk under sliding contact. ASME J. Tribol. **132**, 021901 (2010)
23. Katta, R.R., Polycarpou, A.A., Lee, S.C., Suk, M.: Experimental and FEA scratch of magnetic storage thin-film disks to correlate magnetic signal degradation with permanent deformation. ASME J. Tribol. **132**, 021902 (2010)
24. Karimpoor, A.A., Erb, U., Aust, K.T., Palumbo, G.: High strength nanocrystalline cobalt with high tensile ductility. Scr. Mater. **49**, 651–656 (2003)
25. Piramanayagam, S.N.: Perpendicular recording media for hard disk drives. J. Appl. Phys. **102**, 011301 (2007)